A Tight-Binding Treatment for ^{13}C NMR Spectra of Fullerenes

T. Heine,[†] G. Seifert,[‡] P. W. Fowler,*[,†] and F. Zerbetto[§]

School of Chemistry, University of Exeter, Stocker Road, Exeter, EX4 4QD, U.K.; FB6 Theoretische Physik, Universität-GH Paderborn, Paderborn, D-33095 Paderborn, Germany; and Dipartimento di Chimica, "G. Ciamician", Universitá di Bologna, via F. Selmi 2, 40126 Bologna, Italy

Received: July 7, 1999; In Final Form: August 10, 1999

The DFTB (density-functional based tight-binding) method is used as a basis for simulating ^{13}C NMR spectra of fullerenes and fullerene molecules. Magnetic shieldings are computed as sums of orbital contributions with the IGLO (individual gauge for local orbitals) method. This method is applied to the experimentally characterized fullerenes from C_{60} to C_{84}. With one scaling parameter, qualitative agreement with experimental patterns and discrimination between alternative isomeric possibilities are achieved. A correlation between local geometry and calculated shift for atoms in pentagon sites is reported.

1. Introduction

^{13}C NMR is the major tool for structural characterization of the fullerenes and their derivatives.[1−7] Theoretical treatments of structure and energies of fullerene isomers have been reported by many groups[8−13] and give a general qualitative picture of the factors influencing thermodynamic stability of these cages.[14] Relative energies and geometries close to those predicted by high-level theories are given at modest computational cost by the density-functional based tight-binding method (DFTB).[15−17]

Scanning of many thousands of isomer possibilities is feasible with this approach.[18,19] Calculations of ^{13}C NMR spectra, on the other hand, generally use much more expensive methods and have been applied only to much smaller subsets. The aim of the present work was to implement the calculation of properties such as shieldings in the tight-binding approach, thus bringing comprehensive treatments of fullerenes and other large molecules within reach.

The structure of the paper is as follows. DFTB and its extension to nuclear magnetic shieldings are described (section 2). The new method is applied to the simulation of ^{13}C NMR spectra of experimental and other fullerenes from C_{60} to C_{84} and dimers $(C_{60})_2$ and $(C_{36})_2$. It is found that this tight-binding treatment is of sufficient accuracy to give qualitatively correct spectra and to help distinguish isomeric alternatives (section 3). Simple approaches based on local geometry give useful predictions of the shifts for sites in pentagons and for the overall range of the spectrum (section 4).

2. Method

The DFTB method is based on an LCAO Ansatz for the Kohn−Sham molecular orbitals ψ_i as a combination of basis functions ϕ_ν centered at the atomic sites:

$$\psi_i = \sum c_\nu^i \phi_\nu \tag{1}$$

Several valence atomic orbitals ϕ_ν may correspond to any one site. These may be represented as linear combinations of Slater-type orbitals (DFTB) or Gaussian-type (GTO-DFTB). The expansion coefficients c_ν^i in (2) are found by solving the secular problem

$$\sum_\mu c_\mu^i (F_{\mu\nu} - \epsilon_i S_{\mu\nu}) = 0 \qquad \text{for all } \nu \tag{2}$$

which is expressed in terms of the Kohn−Sham matrix elements $F_{\mu\nu} = \langle\phi_\mu|\hat{T} + V_{\text{eff}}|\phi_\nu\rangle$ and overlap matrix elements $S_{\mu\nu} = \langle\phi_\mu|\phi_\nu\rangle$. The effective potential V_{eff} is approximated as a superposition of atomic contributions, each determined by an LDA-DFT calculation on a fictitious spherical pseudo-atom subjected to an additional potential $(r/r_0)^n$. This extra potential, introduced by Eschrig,[20] has a beneficial effect on binding energies through its compression of the basis functions and electron densities.[15] The valence wave functions and the effective potential are both taken from the pseudo-atomic calculation. It is only necessary to consider two-center elements of the Kohn−Sham matrix[16]

$$F_{\mu\nu} = \begin{cases} \langle\phi_\mu|\hat{T} + V_j + V_k|\phi_\nu\rangle & \text{for } j \neq k \\ \epsilon_\mu & \text{for } \mu = \nu \\ 0 & \text{otherwise} \end{cases} \tag{3}$$

containing the effective potentials V_j, V_k of the atoms j and k that carry functions ϕ_μ and ϕ_ν. In the case of $j = k$, the one-particle energies of the free atom ϵ_μ are used, giving the correct reference energy in the dissociation limit. Restriction to two-center terms leads to a Kohn−Sham matrix similar to empirically parametrized nonorthogonal tight-binding schemes, but all parameters are obtained here consistently from LDA-DFT calculations.

After solving the secular equations for the single-particle energies ϵ_i and eigenstates of the system, the total energy is written as a sum of energies of occupied Kohn−Sham states and a repulsive, short-range, two-particle interaction U:[15,17]

$$E = \sum_i^{\text{occ}} \epsilon_i + {}^1/_2 \sum_{j\neq k} U_{jk}(R_{jk}) \tag{4}$$

Following ref 15, the repulsive energies for the different atom combinations are then derived as universal, short-range poten-

[†] University of Exeter.
[‡] Universität-GH Paderborn.
[§] Universitá di Bologna.

10.1021/jp9923062 CCC: $18.00
Published on Web 10/12/1999

tials by fitting the difference between the sum of Kohn−Sham energies and the LDA cohesive energy for a reference molecule. Response properties such as the nuclear magnetic shielding are defined within a perturbation framework in terms of ground-state and perturbed wave functions. In such calculations, a Gaussian-type basis is more practical than an STO basis because of the ease of evaluation of the necessary integrals. As the normal implementation of DFTB does not use the wave function explicitly, some modification is necessary to produce a set of molecular orbitals (occupied and virtual) for use in further calculations of properties. In GTO-DFTB the atomic orbitals ϕ_μ are expanded in a set of contracted Gaussian-type orbitals (CGTO). To calculate all necessary matrix elements of the Kohn−Sham and overlap matrices, the effective pseudo-atomic potential from eq 3 is expressed by auxiliary functions representing the density and exchange-correlation potential.

For the calculations on the pseudo-atoms, a modified version of the program package AllChem[21] was used, employing a DZV basis set[22] and a VWN exchange-correlation potential.[23] Auxiliary s type GTOs with exponents αd^{-m} with $\alpha = 2000$, $d = 2$ and $m = 1$ (1) 20 was chosen for the charge density, and $\alpha = 500$, $d = 3$, $m = 1$ (1) 10 for the exchange-correlation potential. Integrations used the standard adaptive Gauss−Chebychev grid of AllChem with a tolerance of 10^{-6}. The confinement potential has $r_0 = 2.7$ a_0 and $n = 4$. In this way, the GTO-DFTB method becomes compatible with any conventional wave function-based package for property calculations in quantum chemistry. The ultimate aim is to calculate magnetic shieldings, i.e., the derivatives of local magnetic fields at nuclei $\mathbf{B}^I$, with respect to an external magnetic field $\mathbf{B}$: $\sigma^I_{\alpha\beta} = -\partial B^I_\alpha/\partial B_\beta$. Use of density-functional based schemes for magnetic properties requires some justification, as the Hohenberg−Kohn theorem does not include vector potentials. Rajagopal and Callaway[24] propose a relativistic generalization which leads to an expression for the nuclear magnetic shielding at point I in terms of the magnetic field derivative of the current density at that point. With some approximations[25,26] the normal Rayleigh−Schrödinger expressions for the shielding can be recovered.

A perennial problem with calculation of magnetic properties is that of gauge origin. Given a choice of origin, the shielding splits into a sum of diamagnetic and paramagnetic (perturbed) contributions. Although in an infinite basis their sum is invariant, it can show strong dependence on the origin in a limited basis set. The solution adopted here is the IGLO (individual gauge for local orbitals) approach[27,28] where the occupied molecular orbitals are first transformed to localized functions and for each LMO the centroid of charge is taken as the origin of vector potential. This choice has the advantage of reducing the paramagnetic contribution and hence minimizing sensitivity to basis in the final computed result. Another solution is the use of so-called gauge-including atomic orbitals (GIAO), which have been used in conjunction with DFT for shielding calculations on small molecules.[29]

In our calculations, the IGLO method is the so-called zero-order approximation as implemented in the deMon-NMR package[30,31] was used. Localized molecular orbitals were constructed with the iterative Foster-Boys procedure[32] which gives a relatively strong localization. Convergence, which can be a problem for the large fullerene π system, was improved by adopting the update formula given in ref 33.

In the GTO-DFTB method, only valence orbitals are treated. Fullerenes with their half-full valence shells are favorable cases as their virtual spaces usually span all necessary symmetries of the perturbed molecular orbitals.[34]

The calculated shieldings are transformed into estimates of experimental chemical shifts in two stages. First, in a valence-only treatment the calculated shieldings for fullerenes are subject to a correction for the missing contribution of the 1 s^2 cores. However, to a very good approximation this contribution may be considered as constant for all carbon atoms in the fullerenes, and therefore canceling in the relative chemical shifts.

The second step involves a scaling correction. The raw calculated ^{13}C NMR spectra span too large a range of shifts in comparison to experiment. This feature arises from an overestimation of the spread of the paramagnetic parts of the shieldings. We therefore apply an empirical correction, multiplying the paramagnetic part of all shieldings by a constant factor. This is equivalent to making a correction of the energies of the unoccupied molecular orbitals. It is well-known that approximate DFT treatments, including many LDA and GGA functionals, give poor energies for unoccupied orbitals[35] and more or less sophisticated correction schemes have been proposed.[31] The simple multiplicative factor chosen here is 0.7, as this gives a reasonable value for the sp^2-sp^3 difference in the C_{60} dimer. Fine-tuning of the scaling factor was not attempted, as work on a more fundamental procedure for implementing this correction is in progress. The abbreviation IGLO-DFTB used in the rest of the paper will denote this scaled version of the model.

Some discussion of the expected accuracy of the IGLO-DFTB method is appropriate here. The parameters of DFTB are obtained using an LDA functional. Calculations using LDA/IGLO[30] and LDA/GIAO[29] are reported to give satisfactory agreement with experimental shielding constants for a variety of small molecules. Performance in some well-known problem cases such as F in F_2 and O in H_2 CO can be improved by taking gradient-corrected functionals. This is attributable to changes in one-particle energies. For quantitative agreement with experiment however, further ad hoc corrections to these energies, as mentioned above, are still necessary.[31] In our simplified theory, the paramagnetic scaling factor performs this role.

3. Results

The remainder of the paper reports our results for a series of fullerene molecules. All geometries were optimized using the DFTB method;[15,16] calculated relative energies of isomers will be reported where appropriate. DFTB geometries are generally found to be close to those from LDA calculations and experiment. Extensive comparisons with many other methods have been reported e.g. for the C_{40} fullerenes.[14] At the optimized geometry, the molecular orbitals (occupied and virtual) were calculated with GTO-DFTB and passed to the NMR routines for evaluation of ^{13}C NMR shieldings. Within the NMR package, all valence electrons were treated as a single group in the localization procedure.

3.1. C_{60}. The C_{60} molecule is of icosahedral symmetry and its ^{13}C NMR spectrum contains a single peak. In the experimental literature of higher fullerene spectra the chemical shift of C_{60} is usually reported as a reference signal; systematic differences of ~0.5 ppm are common (e.g. $\delta_{TMS}(C_{60}) = 143.2$ ppm in ref 3 and $\delta_{TMS}(C_{60}) = 142.68$ ppm in refs 1 and 5. The absolute shielding of C_{60} can be estimated within the IGLO-DFTB model. If we use for the 1s core contribution the DFTB value of 199.3 ppm, and the *unscaled* valence-electron shielding of −148.0 ppm, $\sigma(C_{60})$ becomes 51.3 ppm. An extrapolated value from CHF calculations for the absolute shielding is 43 ppm.[34] Schneider et al.[36] calculate 40.43 ppm for the C_{60} cage using GIAO functions. It seems that this version of the IGLO-

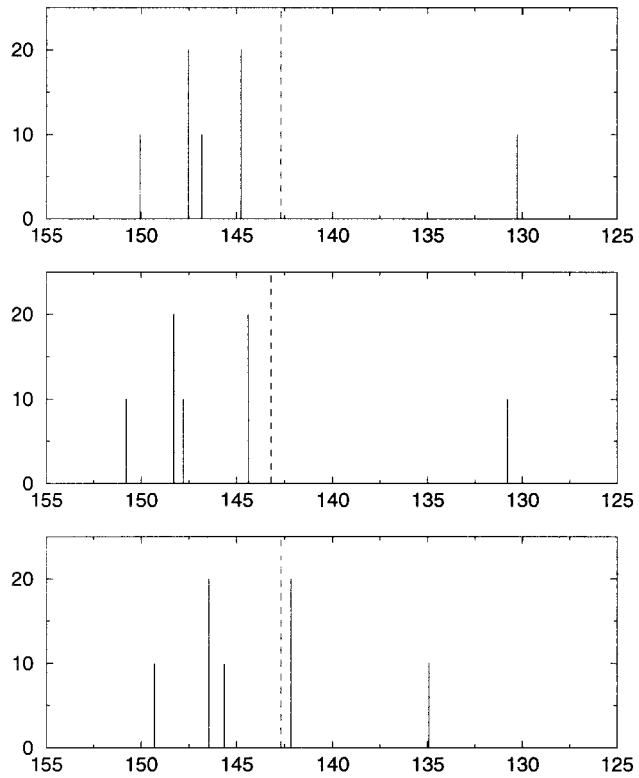

Figure 1. Idealized ^{13}C NMR pattern for D_{5h} C_{70}: (from top to bottom) experiment,[1] experiment,[3] calculation (IGLO-DFTB). Chemical shifts in ppm are shown on the ordinate; peak heights are in atoms per symmetry distinct set. The dashed line indicates the peak for C_{60} within the same experiment or at the same level of theory.

DFTB method produces an error of up to 10 ppm; most of this error is systematic and will disappear when we compare chemical shifts. For the higher fullerenes a *scaled* model is used in order to give a qualitatively reasonable spread of shifts. The calculated spectrum is then shifted to make the C_{60} peak position coincide with experiment. The chemical shifts reported below for each site I are therefore found from

$$\delta_{TMS}(I) = \delta_{TMS}(C_{60}) + \sigma(C_{60}) - \sigma(I) \qquad (5)$$

where $\sigma(I)$ and $\sigma(C_{60})$ are the shieldings in the scaled valence-electron IGLO-DFTB model and $\delta_{TMS}(C_{60})$ is 142.68 ppm.[1] When experimental and calculated spectra are compared in the following, the respective signal for C_{60} is added to each as a dashed vertical line.

3.2. C_{70}. The D_{5h} C_{70} fullerene has an NMR pattern of five peaks, two of them representing 20, and three representing 10 sites (Figure 1). In experiment[1,3] and in DFTB theory the order of the peaks is the same and the spectra are qualitatively similar: a peak of half intensity (10 sites) at ~150 ppm is followed by two peaks, one of full and one of half intensity, both at ~147 ppm; a second peak of full intensity is close to the C_{60} signal and the remaining peak of half intensity is far upfield, by ~14 ppm in experiment and ~10 ppm in the DFTB representation. The overall spread of the spectrum is strongly influenced by this last signal which leads to too small a range in the DFTB pattern. The assignment of the five peaks to atomic sites in IGLO-DFTB corresponds exactly with the interpretation proposed by Taylor et al.[1] and verified by 2D NMR techniques.[2] In IGLO-DFTB the peaks occur at 149.3 (a), 146.5 (c), 145.7 (b), 142.2 (d), and 135.0 ppm (e) where a to e are the distinct sites from cap down to equator. These differ from the observed shifts[1] by 0.7, 1.1, 1.1, 2.5, and 4.7 ppm, respectively. Errors of the order of 5 ppm in chemical shifts may therefore be expected for other fullerenes.

TABLE 1: Relative Energies of C_{78} Fullerenes[a]

N	G	E_{DFTB}	E_{GGA}	E_{HF}	E_{TB}
78:1	D_3	46.1	33.9	31.8	31.1
78:2	C_{2v}	36.8	13.8	27.6	27.4
78:3	C_{2v}	0.0	0.0	0.0	0.0
78:4	D_{3h}	118.7	81.1	88.2	132.5
78:5	D_{3h}	10.6	36.4	32.6	8.4

[a] N gives the name of the isomer in the spiral nomenclature taken from ref 37, G is the point group, E_{DFTB} is the relative energy in the DFTB model. E_{GGA} and E_{HF} are reference values taken from ref 12, where GGA is a full DFT geometry optimization employing a BP86 functional and a 3-21G basis set and E_{HF} are SCF/DZ calculations on MNDO geometries. E_{TB} are tight-binding energies taken from ref 9. All energies are given in kJ mol^{-1} and are relative to the most stable isomer treated at the same level of theory.

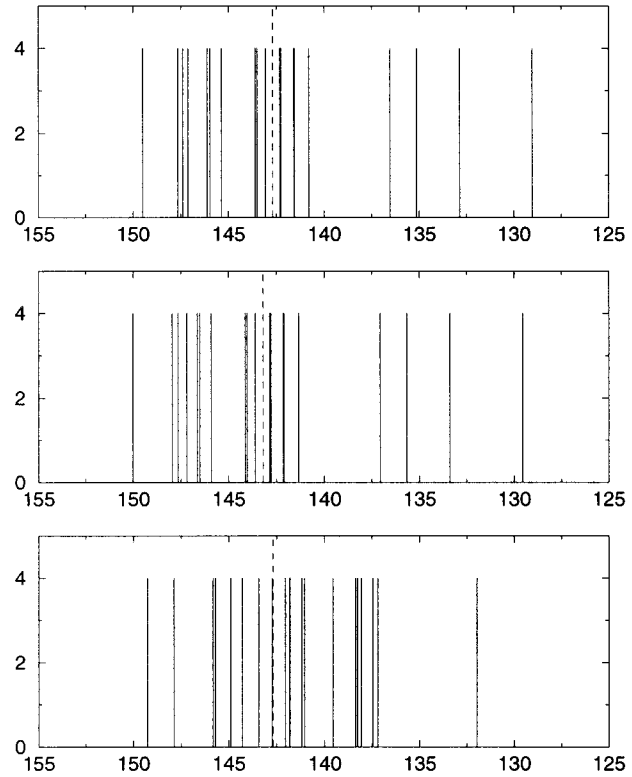

Figure 2. Idealized ^{13}C NMR pattern for D_2 C_{76}: (from top to bottom) experiment,[5] experiment,[3] calculated (IGLO-DFTB). Conventions are as in Figure 1.

3.3 C_{76}. Of the two mathematically possible IPR C_{76} fullerenes one has been characterized in experiment. This is a D_2 cage (76:1 in the spiral notation[37]) and has 19 peaks of equal intensity in the idealized ^{13}C NMR spectrum. Such a pattern is not very informative and within the errors expected the theoretical and experimental pattern are indistinguishable. The spread of the experimental pattern is 20.46 ppm, whereas in IGLO-DFTB it is 17.3 ppm. As in C_{70}, this spread is dominated by a single upfield peak. The three spectra are compared in Figure 2. The IGLO-DFTB spectrum has peaks at 149.3 (3), 147.9 (2), 145.8 (5), 145.7 (15), 144.9 (12), 144.3 (1), 143.4 (13), 142.7 (14), 142.0 (4), 141.8 (16), 141.2 (11), 141.1 (30), 139.5 (17), 138.4 (32), 138.3 (33), 138.1 (19), 137.5 (29), 137.2 (31), and 132.0 (18) ppm, where the label in parentheses specifies the first site in each set of four when atoms are

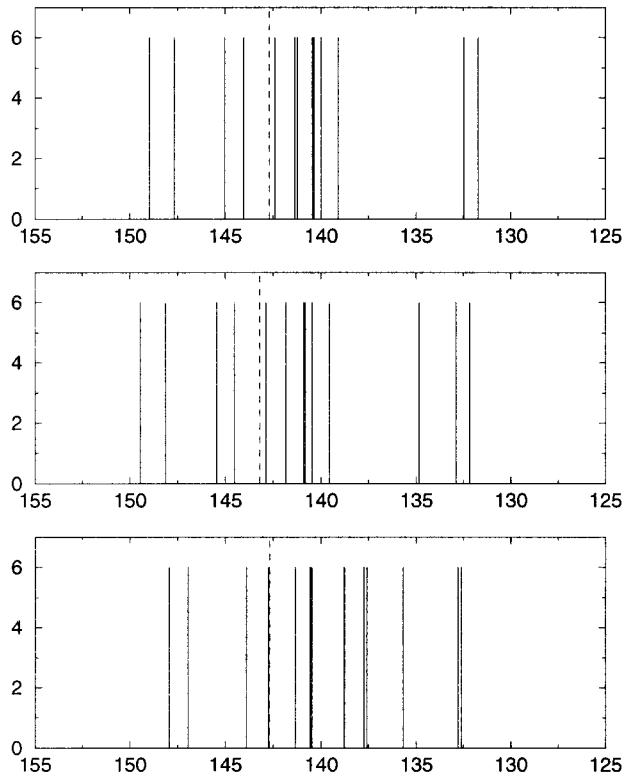

Figure 3. Idealized ^{13}C NMR pattern for D_3 C_{78} (78:1): (from top to bottom) experiment,[5] experiment,[3] calculated (IGLO-DFTB). Conventions are as in Figure 1.

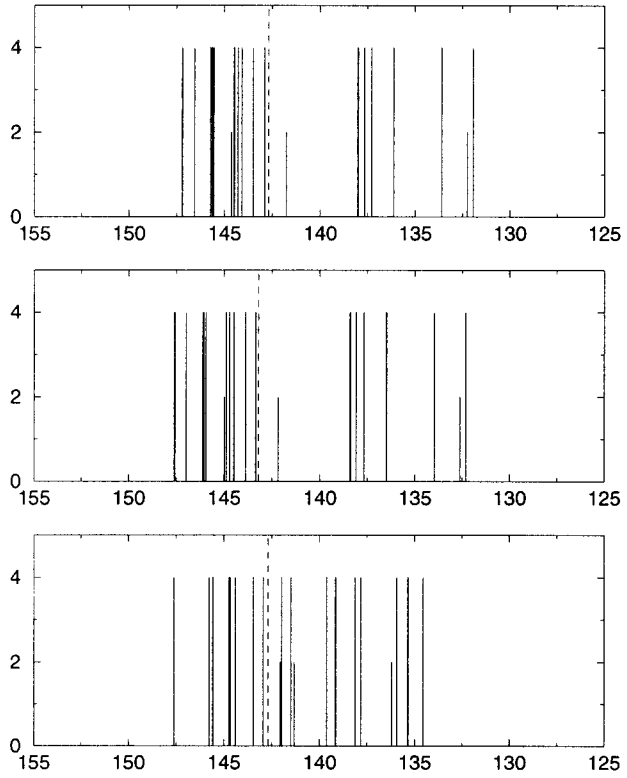

Figure 4. Idealized ^{13}C NMR pattern for C_{2v} C_{78} (78:2): (from top to bottom) experiment,[5] experiment,[3] calculated (IGLO-DFTB). Conventions are given in Figure 1.

numbered according to the IUPAC conventions (see Figure 4 of ref 38).

3.4. C_{78}. There are five mathematically possible IPR isomers of C_{78}; their graphs are of D_3, $2 \times C_{2v}$, and $2 \times D_{3h}$ symmetry.[37] Diederich et al. isolated the D_3 (78:1) and a C_{2v} (78:2) isomers,[3] whereas Taylor et al.[5] and others[39,40] report additionally a third isomer of C_{2v} symmetry (78:3). Table 1 compares the relative energies of the five IPR isomers from the present DFTB optimizations with literature values. All calculations agree that 78:3 has the lowest energy, and perhaps surprisingly, that one of the D_{3h} structures falls in the same energy range as the three experimentally characterized forms. The D_3 isomer (78:1) has 13 signals of equal intensity in the idealized ^{13}C NMR spectrum. The calculated spectrum contains peaks at 147.9 (2), 147.0 (1), 143.9 (7), 142.7 (9), 141.3 (10), 140.6 (8), 140.5 (22), 138.8 (11), 137.7 (26), 137.6 (24), 135.7 (27), 132.8 (23), and 132.6 (25) ppm, where the label in brackets specifies the first site in each set of six when atoms are numbered according to the IUPAC convention (see Figure 7 of ref 38). The experimental spectra for this isomer given in refs 3 and 5 differ only in the assignment of one peak. All three spectra are compared in Figure 3. The qualitative structure common to both experimental spectra, with pairing of peaks at both ends of the spectrum and bunching around the C_{60} resonance, is satisfactorily reproduced in the calculation. The spread of the experimental spectrum is 17.24 ppm[5] (17.27 ppm[3]) compared with 15.32 ppm (calculated, IGLO-DFTB).

The C_{2v} isomer 78:2 has three peaks of half and 18 peaks of full intensity. In our calculation peaks occur at 147.6 (1), 145.8 (2), 145.6 (10), 145.6 (26), 144.7 (12), 144.7 (9), 144.4 (28), 143.5 (11), 143.0 (27), 142.1* (39), 142.0 (25), 141.5 (8), 141.3* (13), 139.6 (22), 139.2 (5), 138.1 (20), 137.8 (29), 136.2* (30), 135.9 (7), 135.4 (24), and 134.6 (23) ppm, where the labels refer to Figure 6 of ref 38 and an asterisk refers to half intensity. Again, the calculated spectrum is qualitatively similar to the experimental, with some compression of the range (experiment: 15.28 ppm,[5] 15.31 ppm,[3] IGLO-DFTB: 13.05 ppm). Inspection of the three-half-intensity peaks shows for example that IGLO-DFTB correctly finds two near the C_{60} line and one upfield, but appears to underestimate the distance between the upfield peak and the downfield pair. The three spectra are given in Figure 4.

The second, and more stable, C_{2v} isomer (78:3) has five signals of half and 17 signals of full intensity. Calculated peaks are at 146.8 (9), 146.6 (10), 146.0 (1), 144.2 (26), 143.6* (33), 142.5* (27), 142.1* (34), 141.3 (8), 141.2* (18), 141.2 (35), 140.6 (25), 140.6 (36), 140.4 (16), 139.3 (22), 138.6 (4), 137.5 (15), 137.2 (17), 137.1 (3), 136.6* (37), 136.0 (24), 135.1 (23), and 134.3 (7) ppm using the IUPAC labeling from Figure 8 of ref 38. The calculated and experimental spectra show some similarity, though with some compression in the IGLO-DFTB spectrum and underestimation of the distance between the half-intensity peaks near the C_{60} line. The spread of the spectrum is 12.48 (IGLO-DFTB) vs 14.77 ppm (experiment[5]). The two spectra are compared in Figure 5. One important use of calculated spectra is in helping to distinguish isomeric possibilities. Symmetry and connectivity determine the number and intensity of the peaks; even a qualitative indication of the chemical shifts may then be enough to decide between isomers with the same peak count. For example, Figure 6 compares the calculated spectra of the remaining D_{3h} IPR isomers of C_{78}. The spectra both have five full and three half-intensity peaks, but are quite different in appearance. The spectrum of the high-energy egg-shaped (leapfrog) isomer 78:4 is spread over 11.5 ppm, and that of the more stable, rounded isomer 78:5 occupies only half this range. In detail, the calculated chemical shifts for 78:4 are (labeled as in Figure 5 of ref 38) 147.6 (1), 144.1 (22), 143.8 (7), 143.5 (10), 141.6* (8), 141.4* (27), 138.0 (23),

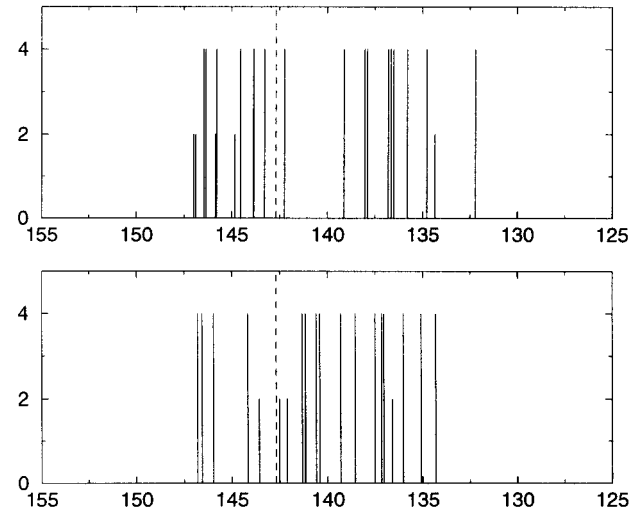

Figure 5. Idealized ^{13}C NMR pattern for C_{2v} C_{78} (78:2): (from top to bottom) experiment,[5] experiment,[3] calculated (IGLO-DFTB). Conventions are given in Figure 1.

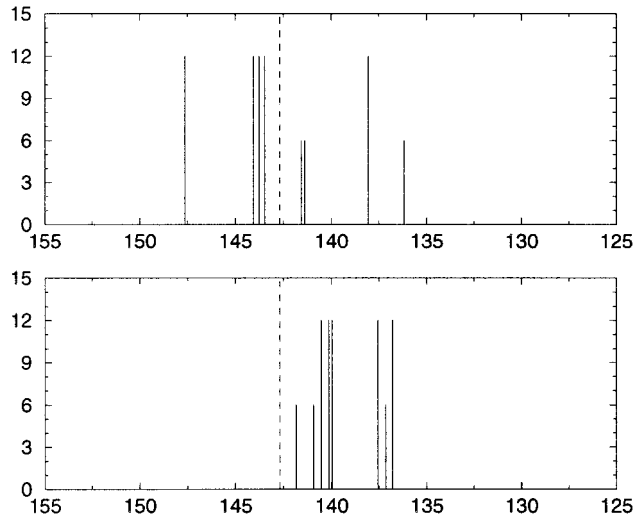

Figure 6. NMR pattern for the two D_3 C_{78} isomers: (from top to bottom) 78:4 and 78:5 in the IGLO-DFTB model. Conventions as in Figure 1.

and 136.2* (24) ppm. For 78:5 they are (see Figure 9 in ref 38 for labeling) 141.8* (27), 140.9* (8), 140.5 (23), 140.1 (10), 140.0 (22), 137.6 (1), 137.1* (24), and 136.8 (7) ppm.

3.5. C_{84}. C_{84} is a higher fullerene for which assignment of the experimental isomers has provoked some discussion. The major C_{84} fraction from the synthesis contains a 2:1 mixture of two isomers, one of D_2 and one of D_{2d} symmetry.[4,5,41] There are 24 mathematically possible IPR isomers of C_{84}: 1 C_1, 5 C_s, 5 C_2, 4 C_{2v}, 4D_2, 2 D_{2d}, 1 D_{3d}, 1 D_{6h}, and 1 T_d. The D_{2d} isomers can be distinguished by their connectivities, and the experimental D_{2d} isomer is therefore identified as 24:23. All D_2 isomers would have 21-line spectra with all lines of equal intensity. Arguments for the identity of the experimental D_2 isomer have been based on energy,[8,9] isomer ratio,[41] growth mechanism,[42] and the ^{13}C NMR spectrum itself.[36] Calculations of the relative energies by a variety of methods all agree in finding the pair of isomers D_{2d} 84:23 and D_2 84:22 to be lowest in the set, with a splitting of 5 kJ mol^{-1} or less (see Table 2). It has been proposed that the 2:1 D_2:D_{2d} ratio found in the C_{84} fraction from several experimental groups represents a statistical symmetry factor, characteristic of two quasi isoenergetic isomers interconverted by a single Stone−Wales transformation step.[43] This assignment

TABLE 2: Relative Energies of C_{84} Optimized Geometries[a]

N	G	E_{DFTB}	E_{GGA}	E^*_{HF}	E_{SCF}	E_M	E_{TB}
84:1	D_2	229.1				241.3	123.2
84:5	D_2	66.5			97.9	96.6	
84:21	D_2	55.1		109.1		68.5	
84:22	D_2	0.0	0.0	0.0	0.0	0.0	0.0
84:23	D_{2d}	1.4	−5.3	−0.3	−1.7	−1.7	3.18

[a] E_M are MNDO energies from ref 11. E_{TB} are tight-binding energies taken from ref 9. Conventions and symbols are as in Table 1, except E_{SCF} are full optimized SCF energies from ref 36, the E^*_{HF} energies refer to frozen MNDO geometries and E_M are MNDO energies from ref 11.

of the experimental isomer as 84:22 was given further support by ab initio calculations on the ^{13}C NMR spectra of isomers 84:5, 84:22, and 84:23.[36] Wakabayashi et al. had claimed 84:5 for the D_2 isomer as this would be compatible with a ring-stacking model of fullerene formation.[42] However, Schneider et al. conclude that isomer 84:5 can be ruled out on the grounds of the width of its calculated spectrum. The IGLO-DFTB method offers the possibility of making a wider comparison, taking into account all D_2 isomers. The available experimental ^{13}C NMR spectra for C_{84} are composites, containing lines from both D_{2d} and D_2 isomers, which because of the 2:1 stoichiometric ratio give rise to a set of 31 lines of full intensity and one line of half intensity. Only this half-intensity line can be assigned with certainty to one of the isomers. However, the narrow range of the spectrum (10.23 ppm) provides an important clue as we will see below. Figure 7 presents the IGLO-DFTB calculated spectra for the D_{2d} and the four D_2 isomers, and compares them with those calculated by Schneider et al.[36] and with the composite experimental spectrum.[5]

In detail, the calculated shifts are as follows (in ppm): **84:23** in ref 38): 142.9 (1), 141.4 (2), 139.9 (9), 139.9 (21), 138.8 (8), 138.2* (32), 137.9 (5), 137.6 (23), 137.0 (7), 136.7 (12), and 133.9 (13); **84:22** (Figure 10 in ref 38): 141.8 (8), 141.5 (23), 141.3 (13), 141.1 (1), 140.9 (25), 140.8 (11), 140.6 (12), 140.4 (3), 140.3 (2), 140.1 (9), 140.1 (31), 140.1 (32), 139.9 (24), 138.8 (14), 137.7 (10), 137.5 (7), 136.8 (29), 136.4 (30), 134.8 (26), 134.8 (27), and 133.1 (28); **84:1**: 153.1, 151.7, 149.2, 148.6, 148.6, 147.3, 147.1, 146.0, 145.9, 145.4, 144.7, 142.4, 141.7, 138.8, 138.2, 136.6, 135.8, 135.5, 133.1, 132.7, and 132.5; **84:5**: 150.2, 145.3, 144.8, 144.0, 143.4, 142.0, 140.8, 140.3, 140.1, 139.8, 139.2, 138.8, 138.1, 138.0, 137.7, 137.7, 137.5, 137.3, 136.4, 135.3, and 132.3; **84:21**: 141.9, 141.2, 140.3, 140.2, 139.4, 139.1, 138.8, 138.8, 138.6, 138.4, 138.3, 137.4, 137.0, 136.4, 136.5, 134.7, 134.0, 133.5, 133.1, 132.7, and 130.6.

It can be seen that both calculations give similar D_{2d} spectra, fitting well within the experimental range and agreeing on the central position of the half-intensity line. The D_2 isomers fall into two sets. Isomers 84:1 and 84:5 have several peaks far downfield of C_{60}, and outside the experimental range. Isomer 84:5 is even more strongly disfavored by the GIAO results from ref 36, but again the qualitative similarity of the IGLO-DFTB and ab initio model spectra is encouraging. The spectrum of isomer 84:22 fits comfortably inside the experimental range, a conclusion that is again in agreement with the ab initio calculations. However, it should be pointed out that 84:21 also has a relatively narrow spectrum and cannot be ruled out on grounds of this comparison alone. Energetic factors favor 84:22 over 84:21. Thus, the calculated energies and spectra taken together support the assignment of the major C_{84} fraction to a 2:1 mixture of 84:22 and 84:23.

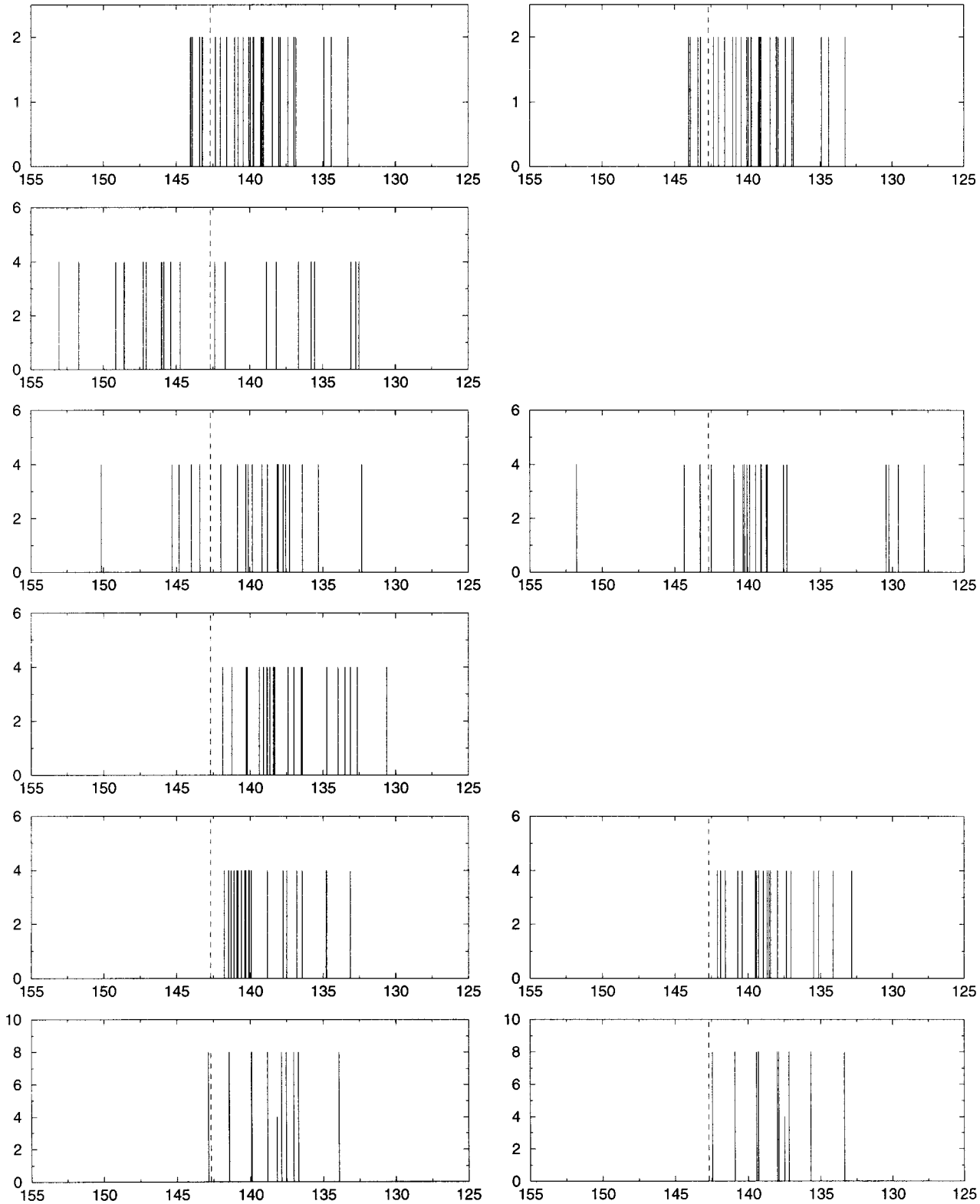

Figure 7. NMR patterns for C_{84} isomers: The left-hand column shows (top to bottom) experimental spectrum of the mixture,[5] IGLO-DFTB calculated spectra for isomers 84:1, 84:5, 84:21, 84:22, and 84:23. On the right are shown GIAO−SCF calculated spectra[36] for isomers 84:5, 84:22 and 84:23. Conventions are as in Figure 1.

The authors of ref 36 did not calculate a spectrum for 84:1, but predicted from a simple geometrical correlation that this cage would have a large range of shifts. Our calculations have confirmed this expectation and the use of correlations of this kind will be explored in more depth below.

There is evidence for a large number of minor isomers of C_{84} at much lower abundance in the experimental product.[5,44] A full survey of model spectra of all 24 IPR isomers will be reported elsewhere.

3.6. Fullerene Dimers: $(C_{60})_2$. The C_{60} dimer is a well characterized species, with both an X-ray structure and ^{13}C NMR spectrum reported in ref 6. It offers an opportunity to test the performance of the IGLO-DFTB model for systems that include both sp^3 and sp^2 carbon sites. In the dimer the two fullerene

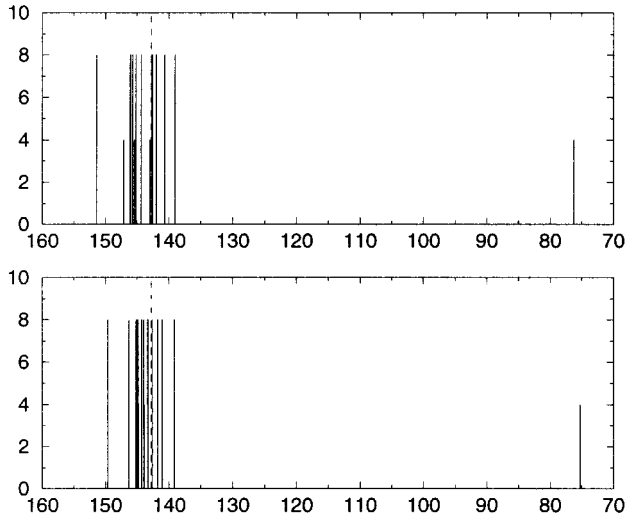

Figure 8. NMR pattern for $(C_{60})_2$: (from top to bottom) experiment,[6] calculated (IGLO-DFTB). Conventions are as in Figure 1.

cages are linked by a bridging four-membered ring, with consequent reduction of the symmetry to D_{2h}. The atoms fall into 13 orbits of eight and four orbits of four, going a 17-line spectrum with four lines of half intensity. A convenient way to label the 17 orbits is by their coordinate on the dimerization axis, counting outward from the sp^3 bridging sites on each ball. The DFTB optimum geometry of the bridged dimer has already been reported[45] and was used here without further change. The calculated spectrum (Figure 8) does indeed give a sharp separation between the chemical shift of the bridging sp^3 atoms (calculated 75.3 ppm, measured 76.22 ppm). The remainder of the calculated spectrum is also in qualitative agreement with the experimental. Most of the peaks cluster around the position of the unperturbed C_{60} line; the IGLO-DFTB range is as usual somewhat more compressed. Computed chemical shifts, labeled as described above, are 149.6 (2), 146.3 (4), 145.3* (17), 145.2 (13), 145.0 (7), 144.8 (16), 144.8* (8), 144.3 (11), 143.9 (15), 143.9* (10), 143.3 (14), 142.6 (12), 142.6 (9), 141.8 (6), 141.1 (5), 139.1 (3), and 75.3* (1) ppm.

3.7. Fullerene Dimers: $(C_{36})_2$. The announcement of the synthesis of C_{36}, which would be the first experimentally characterized fullerene with adjacent pentagons to be found, has provoked considerable discussion.[7,18,46−51] One of the key pieces of evidence presented[7] for the identification of the cage as the cylindrical isomer 36:15 was a ^{13}C NMR powder spectrum. Although the simplicity of the experimental spectrum could be taken as an indication of high symmetry, in fact the isolated molecule 36:15 would be expected to undergo Jahn−Teller distortion. Perhaps more significantly, the powder spectrum shows no sp^3 peaks, although the molecule would be expected to form covalent linkages in the solid. Band gap measurements on thin films of the same material, for example, were interpreted as evidence of clustering of C_{36} molecules in dimers or trimers on gold surfaces.[46] Of all the lower fullerene isomers, 36:15 is predicted to have the greatest tendency to covalent bond formation, and its dimerization energy is predicted in the DFTB model to exceed that of C_{60} by a factor of 10.

In view of these conflicting pieces of evidence, it is of interest to predict the ^{13}C NMR spectrum of the C_{36} dimer and to check the position of the sp^3 peak. This was done within the IGLO-DFTB model. The optimized geometry for the D_{2h} dimer is taken from ref 18. As Figure 9 shows, the spectrum has a normal sp^3 peak, as expected[18] and the sp^2 region shows an asymmetric distribution of intensity, with the lower intensity at higher

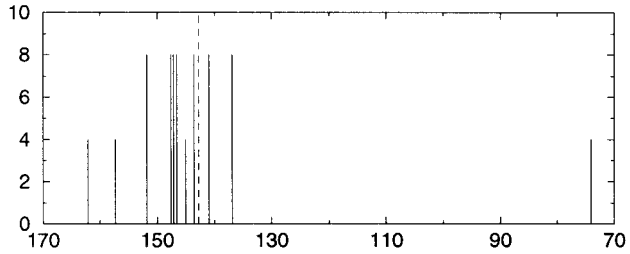

Figure 9. NMR pattern for $(C_{36})_2$: calculated (IGLO-DFTB). Conventions as in Figure 1.

TABLE 3: Correlation of Chemical Shift and Environment on Diederich and Whetten's Model (Ref 3)[a]

	G	L
70:1	D_{5h}	11123
76:1	D_2	11111 11112 22223 3323
78:1	D_3	11111 13222 332
78:2	C_{2v}	11121 12111 32221 33323 2
78:3	C_{2v}	11121 11222 23321 32133 22
78:4	D_{3h}	12112 133
78:5	D_{3h}	12232 132
84:1	D_2	11121 11211 12133 22333 3
84:5	D_2	11111 32213 22222 33223 3
84:21	D_2	13232 22332 22211 32213 2
84:22	D_2	22223 23232 11311 12332 2
84:23	D_{2d}	23132 11223 2

[a] Symbols 1−3 are the pyracylene, corannulene, and pyrene environments discussed in the text and *L* is a string representing the spectrum in descending order of chemical shift. C_{70}:1 represents a perfect correlation; all others are scrambled to a greater or lesser degree.

chemical shift. In detail, the calculated chemical shifts of $(C_{36})_2$ are 162.1* (11), 157.3* (3), 151.8 (5), 147.6 (4), 147.1 (2), 146.5 (8), 143.5 (6), 145.0* (9), 140.9 (10), 136.9 (7), and 74.0* (1) ppm. The atoms are labeled as in the case of the C_{60} dimer from the bridge outward. In a solid the number of sp^3 sites per cage would be expected to increase, and the intensity distributions of the sp^2 part of the spectrum could change significantly. The experimental spectrum apparently has no sp^3 peak.

4. Local Geometry and Chemical Shift

Several schemes have been proposed for correlation of chemical shifts with local environment of the carbon sites in fullerenes. Diederich and Whetten[3] distinguish between three types of carbon site in fullerenes: the pyracylene site (1) where the atom is in one pentagonal ring and joined by an exo bond to a second; the corannulene site (2) where the atom is in a pentagonal ring and joined by an exo bond to a hexagon; the pyrene site (3) where the atom lies at the fusion of three hexagonal rings. The suggestion in ref 3 is that signals from sites (1) should appear at ∼150 ppm, from sites (3) at ∼130 ppm and from sites (2) somewhere in between. This idea was tested on the IGLO-DFTB calculated spectra of all twelve isomers discussed in this paper. Table 3 summarizes the results, showing the occurrence of the different site types in the ordered lists of peaks. The lists do indeed resemble the ideal strings (1...1) (2...2) (3...3) for the smaller fullerenes but become more and more scrambled for the higher atom counts.

A more quantitative proposal attempts to correlate chemical shift in the fullerenes with the local strain as expressed by Haddon's POAV1 angle.[52] In Haddon's model, the π orbital axis vector is defined as that vector which makes equal angles with all three σ bonds to the conjugated site, and the pyramidalization angle (POAV1) is found by subtracting 90° from this common angle. Schneider et al.[36] reported an approximate linear

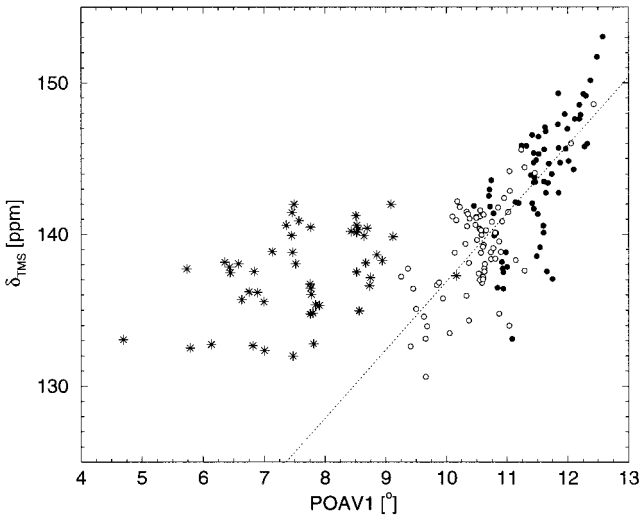

Figure 10. Scatter diagram of POAV1 against chemical shift. Carbon atoms at pyracylene sites are indicated with a full circle, on corannulene sites with an empty circle, and on pyrene sites with a star. The dotted line gives the correlation between the chemical shift at pentagon sites and POAV1: δ_{TMS}/ppm = (4.5 ± 0.3) (POAV1/°) + (91.9 ± 3.4)with a regression coefficient r = 0.78.

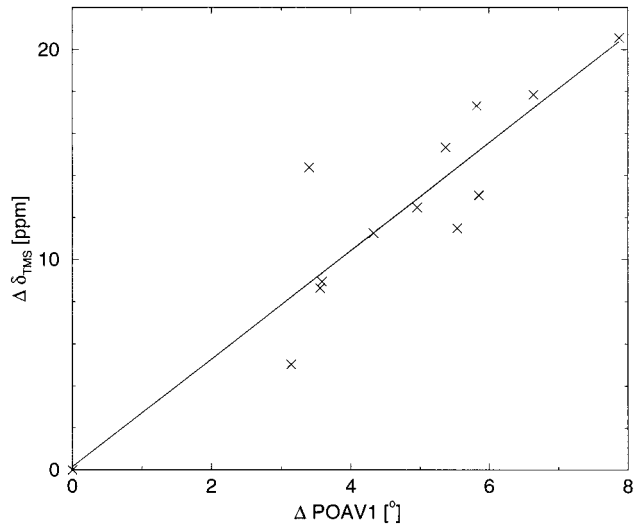

Figure 11. Scatter diagram of the spread of POAV vs that of chemical shift. The fitted line is $\Delta(\delta_{TMS}$ /ppm) = (2.57 ± 0.35))(ΔPOAV1/°) + (0.15 ± 1.73) with a regression coefficient r = 0.91.

correlation between POAV1 angles and total shieldings in isomers 84:5, 84:22, and 84:23. This correlation was used to eliminate isomer 84:1 from consideration, as mentioned earlier.

Our IGLO-DFTB calculations on the same set of isomers give a similarly rough correlation. When the larger dataset of all sites in all isomers treated in the present paper is used, the apparent linearity of the earlier correlation disappears. Figure 10 shows the scatter plot of chemical shift against POAV1. A correlation can be recovered by combining the schemes from refs 3 and 36. When different symbols are used to denote environments 1−3, it becomes clear that the scatter hides two groups of chemical shifts. If we take atoms in pentagonal sites (types 1 and 2), there is a marked upward trend of chemical shift with increasing POAV1 angle. For the pyrene-like sites (3), on the other hand, the angles and shifts are essentially independent. This difference between pentagonal and hexagonal sites is perhaps only to be expected on electronic grounds. The calculated chemical shifts for the pentagonal sites fit a correlation with the POAV1 angles and the spread of the whole ^{13}C NMR pattern also correlates approximately with the spread of POAV1 values (Figure 11).

5. Conclusion

^{13}C NMR spectra calculated using the IGLO-DFTB model are in satisfying qualitative agreement with experiment and with much more expensive theoretical treatments. The model allows the exploration of a wide range of fullerene isomers and reveals some useful correlations. In particular, when assigning spectra, the width of the calculated pattern often allows an isomer to be eliminated from further consideration, even if otherwise compatible with the experimental data in symmetry and numbers and intensities of peaks. It will be applied to the full set of C_{84} isomers and to fullerene derivatives in the near future. The approach is not limited to ^{13}C NMR, and work on e.g. ^{31}P and ^{29}Si spectra of clusters is planned.

Acknowledgment. The authors are grateful to A. M. Köster for his support in programming GTO-DFTB and V. G. Malkin and O. L. Malkina for helpful discussions. The EU TMR scheme is thanked for financial support under contract FMRX-CT96-0126 on Usable Fullerene Derivatives.

References and Notes

(1) Taylor, R.; Hare, J. P.; Abdul-Sada, A. K.; Kroto, H. W. *J. Chem. Soc., Chem. Commun.* **1990**, 1423.
(2) Johnson, R. D.; Meijer, G.; Salem, J. R.; Bethune, D. S. *J. Am. Chem. Soc.* **1991**, *113*, 3619.
(3) Diederich, F.; Whetten, R. L. *Acc. Chem. Res.* **1992**, *25*, 119.
(4) Kikuchi, K.; Nakahara, N.; Wakabayashi, T.; Suzuki, S.; Shiromaru, H.; Miyake, Y.; Saito, K.; Ikemoto, I.; Kainosho, M.; Achiba, Y. *Nature* **1992**, *357*, 142.
(5) Taylor, R.; Langley, G. J.; Avent, A. G.; Dennis, T. J. S.; Kroto, H. W.; Walton, D. R. M. *J. Chem. Soc., Perkin Trans. 2* **1993**, 1029.
(6) Wang, G.-W.; Komatsu, K.; Murata, Y.; Shiro, M. *Nature* **1997**, *387*, 583.
(7) Piskoti, C.; Yarger, J.; Zettl, A. *Nature* **1998**, *393*, 771.
(8) Raghavachari, K. *Chem. Phys. Lett.* **1992**, *190*, 397.
(9) Zhang, B. L.; Wang, C. Z.; Ho, K. M. *Chem. Phys. Lett.* **1992**, *193*, 225.
(10) Colt, J. R.; Scuseria, G. E. *Chem. Phys. Lett.* **1992**, *199*, 505.
(11) Bakowies, D.; Kolb, M.; Thiel, W.; Richard, S.; Ahlrichs, R.; Kappes, M. M. *Chem. Phys. Lett.* **1992**, *200*, 411.
(12) Bühl, M.; van Wüllen, C. *Chem. Phys. Lett.* **1995**, *247*, 63.
(13) Nishikawa, T.; Kinoshita, T.; Nanbu, S.; Aoyagi, M. *J. Mol. Struct. (THEOCHEM)* **1999**, *462*, 453.
(14) Albertazzi, E.; Domene, C.; Fowler, P. W.; Heine, T.; Seifert, G.; Van Alsenoy, C.; Zerbetto, F. *PCCP* **1999**, *1*, 2913.
(15) Porezag, D.; Frauenheim, T.; Köhler, T.; Seifert, G.; Kaschner, R. *Phys. Rev. B* **1995**, *51*, 12947.
(16) Seifert, G.; Porezag, D.; Frauenheim, T. *Int. J. Quantum Chem.* **1996**, *58*, 185.
(17) Seifert, G.; Jones, R. O. *Z. Phys. D* **1991**, *20*, 77.
(18) Fowler, P. W.; Heine, T.; Rogers, K. M.; Sandall, J. P. B.; Seifert, G. Zerbetto, F. *Chem. Phys. Lett.* **1999**, *300*, 369.
(19) Heine, T.; Fowler, P. W.; Rogers, K. M.; Seifert, G. *J. Chem. Soc., Perkin Trans. 2* **1999**, 707.
(20) Eschrig, H.; Bergert, I. *Phys. Status Solidi B* **1978**, *90*, 621.
(21) Köster, A. M.; Krack, M.; Lebœuf, M.; Zimmermann, B. AllChem, Universität Hannover, 1998.
(22) DZV is the sp part of the standard DZVP basis from Godbout, N.; Salahub, D. R.; Andzelm, J.; Wimmer, E. *Can. J. Chem.* **1992**, *70*, 560.
(23) Vosko, S. H.; Wilk, L.; Nusair, M. *Can. J. Phys.* **1980**, *58*, 1200.
(24) Rajagopal, A. K.; Callaway, K. *Phys. Rev. B* **1973**, *7*, 1912.
(25) Bieger, W.; Seifert, G.; Eschrig, H.; Grossmann, G. *Chem. Phys. Lett.* **1985**, *115*, 275.
(26) Friedrich, K.; Seifert, G.; Grossmann, G. *Z. Phys. D* **1990**, *17*, 45.
(27) Kutzelnigg, W. *Isr. J. Chem.* **1980**, *19*, 193.
(28) Schindler, M.; Kutzelnigg, W. *J. Chem. Phys.* **1982**, *76*, 1919.
(29) Schreckenbach, G.; Ziegler, T. *J. Phys. Chem.* **1995**, *99*, 606.
(30) Malkin, V. G.; Malkina, O. L.; Salahub, D. R. *Chem. Phys. Lett.* **1993**, *204*, 80, 87.
(31) Malkin, V. G.; Malkina, O. L.; Casida, M. E.; Salahub, D. R. *J. Am. Chem. Soc.* **1994**, *116*, 5898.
(32) Foster, J. M.; Boys, S. F. *Rev. Mod. Phys.* **1960**, *32* 296, 303, 305.

(33) Pipek, J.; Mezey, P. G. *J. Chem. Phys.* **1989**, *90*, 4916.
(34) Fowler, P. W.; Lazaretti, P.; Zanasi, R. *Chem. Phys. Lett.* **1990**, *165*, 79.
(35) Savin, A.; Umrigar, C. J.; Gonze, X. *Chem. Phys. Lett.* **1998**, *288*, 391.
(36) Schneider, U.; Richard, S.; Kappes, M. M.; Ahlrichs, R. *Chem. Phys. Lett.* **1993**, *210*, 165.
(37) Fowler, P. W.; Manolopoulos, D. E. *An atlas of fullerenes*; Oxford University Press: New York, 1995.
(38) Taylor, R. *J. Chem. Soc., Perkin Trans 2* **1993**, 813.
(39) Kupfer, M.; Knauff, O.; Golden, M. S.; Fink, J.; Burk, M.; Fuchs, D.; Schuppler, S.; Michel, R. H.; Kappes, M. M. *Chem. Phys. Lett.* **1996**, *258*, 513.
(40) Benz, M.; Fanti, M.; Fowler, P. W.; Fuchs, D.; Kappes, M. M.; Lehner, C.; Michel, R. J.; Orlandi, G.; Zerbetto, F. *J. Phys. Chem.* **1996**, *100*, 13399.
(41) Manolopoulos, D. E.; Fowler, P. W.; Taylor, R.; Kroto, H. W.; Walton, D. R. M. *J. Chem. Soc., Faraday Trans.* **1992**, *88*, 3117.
(42) Wakabayashi, T.; Shiromaru, H.; Kikuchi, K.; Achiba, Y. *Chem. Phys. Lett.* **1993**, *201*, 470.
(43) Stone, A. J.; Wales, D. J. *Chem. Phys. Lett.* **1986**, *128*, 501.
(44) Tagmatarchis, N.; Avent, A. G.; Prassides, K.; Dennis, T. J. S.; Shinohara, H. *J. Chem. Soc., Chem. Commun.* **1999**, 1023.
(45) Porezag, D.; Jungnickel, G.; Frauenheim, T.; Seifert, G.; Ayuela, A.; Pederson, M. *Appl. Phys. A* **1997**, *64*, 321.
(46) Collins, P. G.; Grossman, J. C.; Côté, M.; Ishigami, M.; Piskoti, C.; Louie, S. G.; Cohen, M. L.; Zettl, A. *Phys. Rev. Lett.* **1999**, *82*, 165.
(47) Grossman, J. C.; Côté, M.; Louie, S. G.; Cohen, M. L. *Chem. Phys. Lett.* **1998**, *284*, 344.
(48) Slanina, Z.; Zhao, X.; Osawa, E. *Chem. Phys. Lett.* **1998**, *290*, 311.
(49) Côté, M.; Grossman, J. C.; Cohen, M. L.; Louie, S. G. *Phys. Rev. Lett.* **1998**, *81*, 697.
(50) Heine, T.; Fowler, P. W.; Seifert, G. *Solid State Commun.* **1999**, *111*, 19.
(51) Fowler, P. W.; Mitchell, D.; Zerbetto, F. *J. Am. Chem. Soc.* **1999**, *121*. 3218.
(52) Haddon, R. C.; Scott, L. T. *Pure Appl. Chem.* **1986**, *58*, 137.